

This article was downloaded by: [Tomsk State University of Control Systems and Radio]

On: 23 February 2013, At: 03:05

Publisher: Taylor & Francis

Informa Ltd Registered in England and Wales Registered Number: 1072954

Registered office: Mortimer House, 37-41 Mortimer Street, London W1T 3JH, UK



## Molecular Crystals and Liquid Crystals

Publication details, including instructions for authors and subscription information:

<http://www.tandfonline.com/loi/gmcl16>

### Influence of the Patch Effect and Near - Contact Trapped Charge on Electrode - Limited Current Flow in Molecular Crystals

J. Godlewski<sup>a</sup>

<sup>a</sup> Institute of Physics, Technical University of Gdańsk, Gdańsk, Poland

Version of record first published: 20 Apr 2011.

To cite this article: J. Godlewski (1981): Influence of the Patch Effect and Near - Contact Trapped Charge on Electrode - Limited Current Flow in Molecular Crystals, Molecular Crystals and Liquid Crystals, 71:1-2, 19-33

To link to this article: <http://dx.doi.org/10.1080/00268948108072715>

PLEASE SCROLL DOWN FOR ARTICLE

Full terms and conditions of use: <http://www.tandfonline.com/page/terms-and-conditions>

This article may be used for research, teaching, and private study purposes. Any substantial or systematic reproduction, redistribution, reselling, loan, sub-licensing, systematic supply, or distribution in any form to anyone is expressly forbidden.

The publisher does not give any warranty express or implied or make any representation that the contents will be complete or accurate or up to date. The accuracy of any instructions, formulae, and drug doses should be

independently verified with primary sources. The publisher shall not be liable for any loss, actions, claims, proceedings, demand, or costs or damages whatsoever or howsoever caused arising directly or indirectly in connection with or arising out of the use of this material.

# Influence of the Patch Effect and Near-Contact Trapped Charge on Electrode-Limited Current Flow in Molecular Crystals†

J. GODLEWSKI

*Institute of Physics, Technical University of Gdańsk, Gdańsk, Poland‡*

(Received April 18, 1980; in final form July 28, 1980)

The problem of the discrepancies between the theoretical value of the Schottky factor  $a_{th} = e/kT(e/4\pi\epsilon\epsilon_0)^{1/2}$  and its experimental values has been examined for electrode-limited (ELC) in molecular crystals. It is concluded that the patch effect as well as discretely distributed near-contact charge are responsible for the factor  $a$ . The problem has been considered for both metallic and electrolytic electrodes. The predicted qualitative behaviour of the factor  $a$  has been proved to be in good agreement with deviations of  $a$  observed in experiment.

## 1 INTRODUCTION

The currents observed in thin organic crystals for high electric fields are often electrode-limited-currents (ELC). To explain ELC voltage characteristics for injection from electrodes with image barrier many authors have applied the Schottky relation<sup>1–11</sup> in the form given by<sup>12,13</sup>

$$j \cong AT^2 \exp\left(-\frac{\phi_0}{kT}\right) \exp(a_{th} E_0^{1/2}) \quad (1)$$

† Research supported in part by the Polish Academy of Sciences under Programm PR-3.

‡ Instytut Fizyki, Politechnika Gdańska, Majakowskiego 11/12 80-952 Gdańsk, Polska.

with

$$a_{th} = \frac{e}{kT} \left( \frac{e}{4\pi\epsilon\epsilon_0} \right)^{1/2}, \quad (1a)$$

where  $A$  is Richardson's constant,  $T$  = absolute temperature,  $\phi_0$  = surface energy of a carrier,  $E_0 = U/d$  = applied electric field,  $e$  = electronic charge,  $\epsilon$  = dielectric constant,  $\epsilon_0$  = vacuum permittivity,  $k$  = Boltzmann's constant. The distance of the Schottky barrier maximum from the electrode surface is given by  $x_{max} = (e/16\pi\epsilon\epsilon_0 E_0)^{1/2}$ . Experimental results for ELC in insulators show that there exist, very often, considerable discrepancies between the theoretical value of the Schottky factor  $a_{th}$  and its experimental values  $a_{exp}$ .<sup>1,3,5,6,11</sup>

The analysis of the curves shown in Figure 1 and other  $j - E_0$  characteristics contained in<sup>1,3,7,10-13,16,22,29,31,44</sup> having in the author's opinion typical features of ELC in the Schottky emission conditions† allows one to formulate the following two statements:

- i)  $a_{exp}$  is greater than  $a_{th}$  in the case of metallic electrodes (sometimes  $a_{exp} > 5a_{th}$  (see Figure 1e)),
- ii)  $a_{exp}$  is equal to<sup>4,10</sup> or less<sup>16</sup> than  $a_{th}$  for electrolytic contacts.‡

Different authors pointed out various reasons for these discrepancies such as: the decrease of the dielectric constant,<sup>11</sup> patch effect<sup>5</sup> or space charge.<sup>1,2,8</sup>

The change of dielectric constant cannot be the main reason of these discrepancies because it would lead to a similar change of  $a_{exp}$  with both metallic and electrolytic electrodes. According to (i) and (ii) it is not the experimental case.

Godlewski and Kalinowski<sup>5</sup> suggested that discrepancies between  $a_{th}$  and  $a_{exp}$  could be the result of the patch effect. The problem, however, was beyond the scope of that paper.

The effect of the space charge on  $a_{exp}$  is not clear. Lengyel<sup>1</sup> suggested that space charge is responsible for the increase of  $a_{exp}$ . Frank and Simmons<sup>2</sup> demonstrated by numerical calculations that space charge does not change  $a$ .

As can be seen from the above outline, the phenomenon is neither completely studied nor is it understood. The aim of this work is to make a contribution to a better understanding of the phenomenon by deriving an expression for the Schottky factor  $a$  taking into account the image force, the patch effect and the space charge accumulated near the injected electrode.

† Theoretical calculations carried out with one-dimensional Onsager theory [17, 18, 19, 24, 43] do not lead to a straight line dependence in  $\log j$  versus  $E_0^{1/2}$  coordinates.

‡ The value of  $a_{exp}$  less than  $a_{th}$  can be obtained after redrawing the data of Figure 1 taken from the paper<sup>16</sup> in  $\log j$  versus  $E_0^{1/2}$  coordinates.

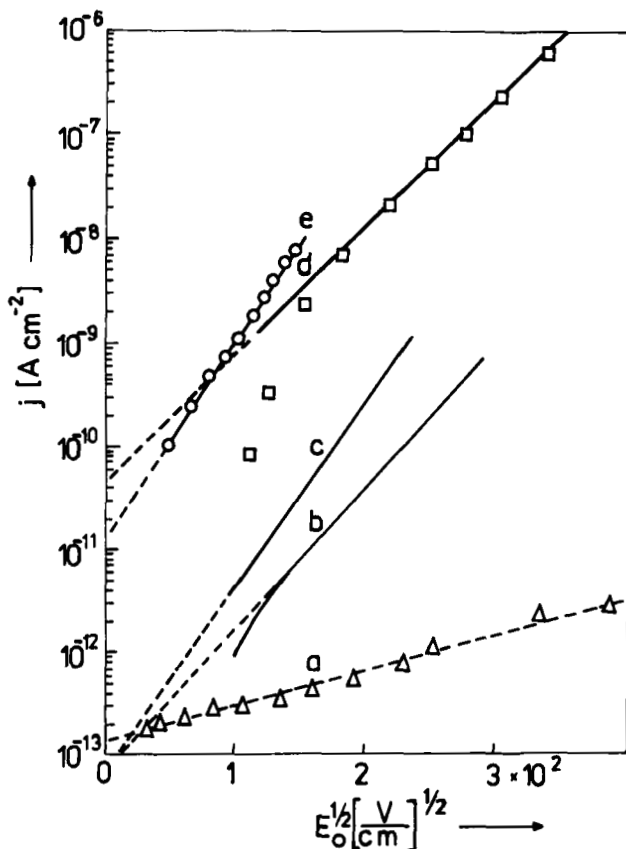


FIGURE 1 Current density  $j$  as a function square root of electric field strength  $E_0^{1/2}$  for some organic crystals: a) anthracene,  $d = 27 \mu\text{m}$ ,  $10^{-3} \text{ M KI}_3$  electrode,<sup>4</sup> b) anthracene, Au electrode,<sup>14</sup> c) perylene,  $d = 24.4 \mu\text{m}$ , Au electrode,<sup>14</sup> d) tetracene,  $d = 22 \mu\text{m}$ , Au electrode, e) pyrene,  $d = 500 \mu\text{m}$ ,  $\text{SnO}_2$  electrode.<sup>15</sup> The slope of curve a) is close to  $a_{\text{th}}$ .

## 2 INFLUENCE OF THE PATCH EFFECT

The analysis of the injection current from a metallic electrode shows that only a small part of the evaporated electrode (a few percent) is active in carrier injection into an insulator<sup>14</sup> (compare with optical properties of discontinuous gold films).<sup>4,5</sup> In visual observation of electroluminescence<sup>20,21</sup> spotted bright luminosity could be observed which indicates that the efficient regions for charge injection from a metallic electrode into an insulator are formed locally. Photographs of evaporated electrodes on organic crystals<sup>14</sup> can serve as an additional confirmation of electrode patched structure.

Since both electrodes could be patched and the work function could vary from one spot to another, the general analysis of such a problem is in fact impossible. Therefore, for the sake of simplicity, let us assume that the active parts of the electrodes have a ring disk shape of  $2R$  diameter and that the work function of every disk is identical (Figure 2).

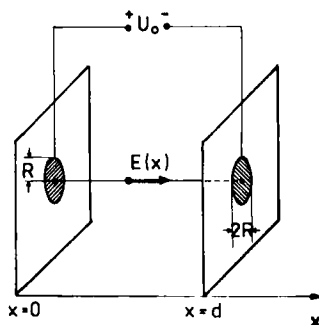


FIGURE 2 Model of patched electrodes. Details in the text.

Assuming, that the potential difference between the two electrode disks is  $U_0 = \int_0^d E(x)dx$ , on the basis of simple electrostatics, we can get an expression for the electric field strength along the axis linking the disk centers,

$$E_{(x)} = \frac{U_0}{2[(d+R) - (d^2 + R^2)^{1/2}]} \left\{ 2 - \frac{x}{(R^2 + x^2)^{1/2}} - \frac{d-x}{[R^2 + (d-x)^2]^{1/2}} \right\} \quad (2)$$

To determine the Schottky factor one has to take into consideration the electric field near the injecting contact ( $x = x_{\max}$  or  $x = d - x_{\max}$ ). It is expected that for high electrical fields, for which  $x_{\max}$  falls in the range of tenth nanometer (see e.g. Ref. 5),  $x_{\max} \ll 2R$  because  $2R$  should be at least of the magnitude of the evaporated crystallites (parts of micron).<sup>14,44</sup> Then, the expression<sup>2</sup> takes the form

$$E_{(0)} = E_{(d)} = \frac{U_0}{2[(d+R) - (d^2 + R^2)^{1/2}]} \left( 2 - \frac{d}{(d^2 + R^2)^{1/2}} \right) = \gamma \frac{U_0}{d} = \gamma E_0 \quad (3)$$

The behaviour of this theoretical expression is plotted in Figure 3. One can easily see that for  $R/d \ll 1$  the electric field  $E_{(0)}$  is much greater than the electric field for the case of planar discontinuous electrodes ( $\gamma \gg 1$ ).

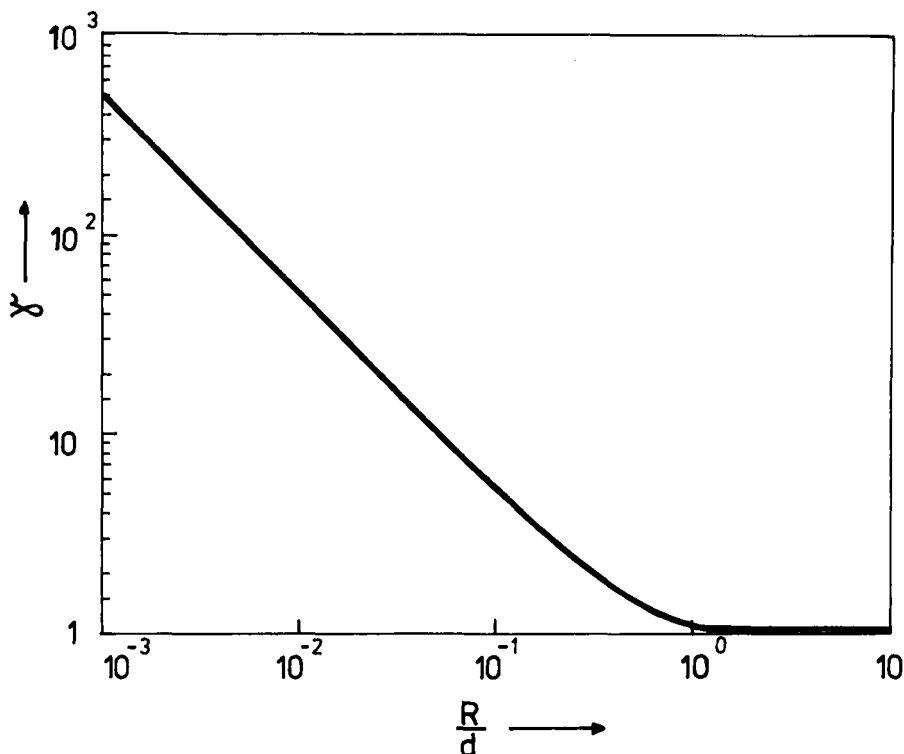


FIGURE 3 Amplification of the near electrode field strength resulting from the patch effect as a function of the ratio  $R/d$ .

If we replace  $E_0$  in Eq. (1a) by  $E_{(0)}$  (3) then the ratio  $a_{\text{exp}}/a_{\text{th}}$  for  $d \gg R$  becomes

$$\frac{a_{\text{exp}}}{a_{\text{th}}} \cong \left( \frac{d}{R} \right)^{1/2} \quad (4)$$

If the distance between individual disks were greater than  $R$  then for such a patched electrode Eq. (4) would give  $a_{\text{exp}}$  much greater than  $a_{\text{th}}$ .

Equation (4) can serve for an estimation of the mean active disk diameter. Applying Eq. (4) to the data of Figure 1 one obtains  $2R$  values of  $1.6 \mu\text{m}$  (b),  $2.4 \mu\text{m}$  (d),  $15 \mu\text{m}$  (c). The dielectric constant taken for calculation was  $\epsilon = 4$ .

Apart from the electrode  $\text{SnO}_2$  for which  $2R = 14 \mu\text{m}$  the other values of  $2R$  are in the range of evaporated crystallite magnitudes.<sup>14,45</sup> If the thickness of a sample is in the range of a few micrometers (e.g. evaporated films) then one can expect  $a_{\text{exp}} \approx a_{\text{th}}$ . Quite a few studies on films for ELC current in Schottky emission conditions confirm this conclusion.<sup>7,22,23,44</sup>

Another argument indicating the influence of the patch effect for metallic electrodes is the value of the Schottky factor for electrolytic electrodes. If the surface Poole–Frenkel effect does not play a role in Schottky emission then for those electrodes  $a_{\text{exp}} \leq a_{\text{th}}$ .<sup>4,10</sup> This is the result of the homogeneity of such contacts. In conclusion, we would like to note, that the patch effect leads to an increase of the Schottky factor compared to its theoretical value.†

### 3 INFLUENCE OF THE DISCRETELY DISTRIBUTED NEAR-ELECTRODE CHARGE

Space charge concentration in the potential barrier region depends on electrode emission efficiency and on trapped charge spatial distribution and concentration. To calculate the influence of the space charge on barrier shape, Poisson's equation is usually applied (see e.g. Ref. 2). However, for the near contact region the discontinuities of charge distribution can determine barrier shape and height. Therefore, we have to take into consideration the fact that trapped charge carriers are discretely distributed among particular points of an insulator. The distance between carriers results from the electrode injection efficiency and the spatial distribution of the trapped charge. The analytical solution of this problem is impossible and the results given in this section are based on some approximations. In the near contact region there exist:

- i) the greatest concentration of free ( $n_f$ ) and trapped ( $n_t$ ) carriers ( $n_f \sim n_t \sim \exp(A/x)$ ),<sup>16,25,27–32</sup>
- ii) the greatest trap concentration ( $H \sim \exp(-Bx)$ ),<sup>33,34</sup>
- iii) a possibility of trapping carriers by tunnelling from the electrode ( $n_t \sim \exp(-Cx)$ ),<sup>5,8</sup>  $A, B, C$ -constants.

According to these assumptions the free and trapped carrier concentrations are strongly decreasing functions with increasing distance from electrode. The inverse process to (iii) and electrode recombination of free carriers lead to removing carriers from near electrode region. Finally, neglecting the contribution from carriers placed in the interior of a sample (for ELC current), we can assume that the barrier shape is defined by the charge lying

---

† In this consideration the electric field was calculated on the axes linking the disk centers. In fact, the charge injection occurs also from other parts of the electrode. In that case the electric field is given by a much more complex expressions. But even in this case  $a_{\text{exp}}$  should be greater than  $a_{\text{th}}$  because of the increase of the electric field near the contact. In general, in random distribution of injecting crystallites with different work function, we could not get a straight line in  $\log j - E_0^{1/2}$  coordinates for ELC currents.



in a narrow layer of the width smaller than the barrier width  $x_{\max}$ . We can admit that this charge is independent of the electric field applied to the sample.

Let us assume that the potential near the contact is determined by discrete positive charges localised at a mean distance  $D/2$  from the electrode. Then, the potential at a distance  $x$  from the electrode, generated by the  $i$ -th charge is given by (see e.g. Figure 4)<sup>26</sup>

$$\varphi_i(x) = \frac{e}{4\pi\epsilon\epsilon_0} \left\{ \frac{1}{[y_i^2 + (x - D/2)^2]^{1/2}} - \frac{1}{[y_i^2 + (x + D/2)^2]^{1/2}} \right\}. \quad (5)$$

The resultant potential  $\varphi(x)$  from all the charges is then

$$\varphi(x) = \sum_{i=1}^n \varphi_i(x), \quad (6)$$

where  $n$  is the number of charges considered.

To find the analytical expression for  $\varphi(x)$  we have to know the space charge distribution near the contact ( $y_i$  for  $i = 1, 2, 3, \dots, n$ ). The potential function is determined mainly by the trapped charge distribution (usually  $n_f \ll n_i$ ).

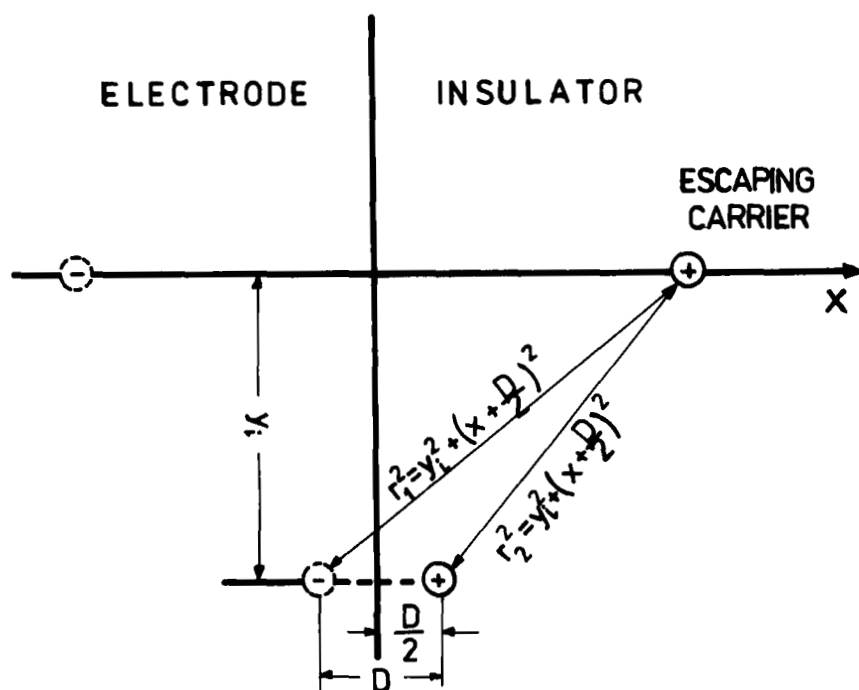


FIGURE 4 Scheme for the calculation of the potential of the  $i$ -th charge.

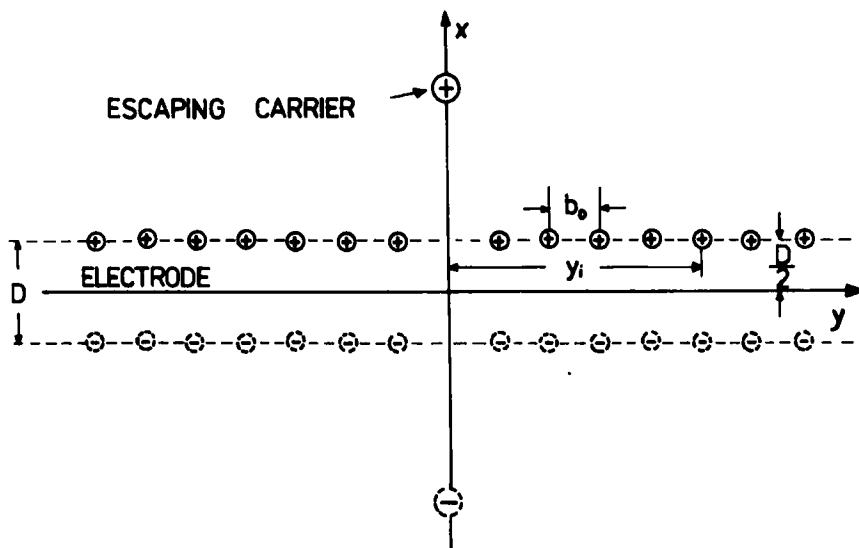


FIGURE 5 Scheme of a linear charge distribution on the plane perpendicular to the electrode.

Therefore, it is important to know the nature of the defect distribution near the electrode; usually deposited on the  $ab$  crystallographic plane. There exist many observations and theoretical analyses pointing out that the distribution of imperfections along  $ab$  plane can be linear.<sup>35,36,37,42</sup>

It might be expected, that the majority of the trapped charge near the surface would be localized along the line parallel to the electrode. That is shown schematically in Figure 5. According to (5) and (6), for linear density of charge ( $\tau$ ) and for  $x > D/2$ , the potential can be expressed by (see Appendix A)

$$\varphi(x) \cong \frac{\tau D}{2\pi\epsilon\epsilon_0 x} \quad \text{with } \tau = \frac{e}{b_0}, \quad (7)$$

where  $b_0$  = distance between the nearest neighbour charges.

It is obvious that linear distribution is not a unique manner in which charges near the contact can be distributed. If the charge in that region is of planar distribution (Figure 6) then a similar procedure (see Appendix B) leads to an approximate expression for the potential ( $x > D/2$ ),

$$\varphi(x) = \frac{\sigma D}{2\epsilon\epsilon_0} \left( 1 - \frac{c_0^2}{2x^2} - 3.55 \frac{c_0^4}{x^4} \right) \quad \text{with } \sigma = \frac{e}{c_0^2}, \quad (8)$$

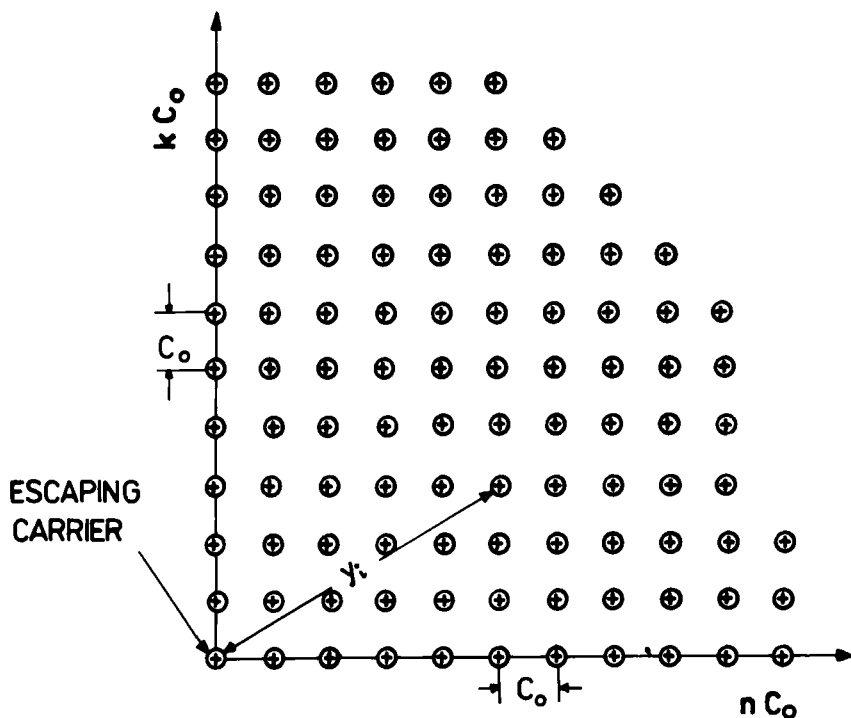


FIGURE 6 Scheme of a planar charge distribution on the plane parallel to the electrode.

where  $\sigma$  = surface density of charge and  $c_0$  = distance between the nearest neighbour charges. In fact, we can expect a much more physically complicated situation. However, it will not be the subject of present analysis.

The mathematical procedure for ELC current density calculation<sup>12,13,25</sup> leads to the Schottky expression ( $j \sim \exp(aE_0^{1/2})$ ) only for the potential given by (7). According to the purpose of the present work we limit our analysis only to the case of linear distribution of the charge in the near electrode region.

Finally, if we take into consideration image forces, patch effect and space charge in the near electrode region in the presence of an external electric field then the expression determining the potential energy of an escaping charge has the form as follows:

$$\phi_{(x)} = \phi_0 - \frac{e^2}{16\pi\epsilon\epsilon_0 x} + \frac{\tau D_e}{2\pi\epsilon\epsilon_0 x} - e\gamma E_0 x. \quad (9)$$

Here  $\gamma = E_{(0)}/E_0$ , is a coefficient determining an increase of electric field due to the patch effect. In this case the position of the potential barrier

maximum is given by the expression

$$x_{\max} = \left[ \frac{(e/8 - \tau D)}{2\pi\epsilon\epsilon_0 \gamma E_0} \right]^{1/2} \quad (10)$$

The value of the coefficient  $a$  is given by

$$a = \frac{e}{kT} \left( \frac{2\gamma}{\pi\epsilon\epsilon_0} \right)^{1/2} \left( \frac{e}{8} - \tau D \right)^{1/2}. \quad (11)$$

When  $\gamma = 1$  and  $\tau \rightarrow 0$ , we get the standard value of the Schottky factor:

$$a = a_{\text{th}} = \frac{e}{kT} \left( \frac{e}{4\pi\epsilon\epsilon_0} \right)^{1/2}. \quad (12)$$

According to Eqs. (1), (9) and (10), the expression determining the current density takes on the form

$$j = j_0 \exp\left(-\frac{\phi_0}{kT}\right) \exp(aE_0^{1/2}), \quad (13)$$

where  $a$  is given by Eq. (11), and  $j_0$  is determined by thermal and optimal injection.<sup>5</sup>

One notes that according to Eqs. (11) and (13), when  $\gamma \gg 1^\dagger$  and  $e/8 \ll \tau D$ ,  $a/8 > a_{\text{th}}$ . Such conditions are typical for metallic electrodes in contact with organic insulators. These electrodes show the patch effect with relatively weak injection (high value of  $\phi_0$ ). If  $\gamma = 1$ , the expression  $(e/8 - \tau D)^{1/2}$  in Eq. (11) determines the value of  $a$  and then  $a < a_{\text{th}}$ . Such conditions are typical for electrolytical contacts, as long as the problem of effective dielectric contact is not important.

From Eqs. (9) to (13) it can be easily shown that in the case of planar distribution it is not possible to obtain an equation of type (13). The  $j - V$  characteristics for such and similar cases would be more complex and will not take on a form of a straight line in  $\log j - E_0^{1/2}$  coordinates. However, in spite of absence of the straight line those currents are also ELC currents.

#### 4 CONCLUDING REMARKS

Experimental data and theoretical considerations presented in this paper explain some of the charge injection mechanisms from the electrode into a real insulator. It is found that in the case of the metallic electrode the effective

<sup>†</sup> For example if  $a_{\text{exp}}/a_{\text{th}} \geq 5$  (Figure 1e) the amplification coefficient  $\gamma \geq 25$ .

value of the Schottky factor  $a$  depends on near-electrode space charge, the patch effect and, of course, the image force.

This dependence is expressed by three factors  $\gamma$ ,  $\tau$  and  $D$  (see (11)).  $\gamma$ , defined as the ratio of the local electric field to its nominal value  $U/d$  (see (9)), is responsible for the inhomogeneity of the electrode creating the patch effect.  $\tau = e/b_0$  and  $D$  characterize the geometrical situation in the crystal near the contact (see Figures 4 and 5) determining the influence of the space charge. On the basis of these considerations it can be seen how the discontinuity of the electrode and near electrode charge distribution influence the  $j - V$  characteristics in organic crystals. Up to now all of the considerations in this field assumed an ideal planar geometry of the electrodes and continuous charge distribution in the space.

### Acknowledgments

The author is greatly indebted to Prof. J. Kalinowski for his continued interest and critical reading of the manuscript. Helpful remarks of Mr J. Gliniski are also acknowledged.

### References

1. G. Lengyel, *J. Appl. Phys.*, **37**, 807 (1966).
2. R. I. Frank and J. G. Simmons, *J. Appl. Phys.*, **38**, 832 (1966).
3. G. R. Johnston, *Chem. Phys. Letters*, **3**, 699 (1969).
4. J. S. Bonham and L. E. Lyons, *Aust. J. Chem.*, **26**, 489 (1973).
5. J. Godlewski and J. Kalinowski, *Phys. Stat. Solidi (a)*, **56**, 293 (1979).
6. J. Godlewski and J. Kalinowski, *Phys. Stat. Solidi (a)*, **56K**, 57 (1979).
7. C. Tantzcher and C. Haman, *Phys. Stat. Solidi (a)*, **26**, 443 (1976).
8. M. Shatzkes, *J. Appl. Phys.*, **49**, 4868 (1978).
9. H. Baessler and H. Killesreiter, *Phys. Stat. Solidi (b)*, **53**, 183 (1972).
10. M. Pope and W. Weston, *Mol. Cryst. Liq. Cryst.*, **25**, 205 (1974).
11. A. M. Goodman, *Phys. Rev.*, **144**, 588 (1966).
12. S. M. Sze, *Physics of Semiconductor Devices* (Wiley, New York, 1969).
13. G. Yepifanov, *Physical Principles of Microelectronics* (Mir Publishers, Moscow, 1974).
14. B. Korsch, F. Willig, H. J. Gaehrs, and B. Tesche, *Phys. Stat. Solidi (a)*, **33**, 461 (1976).
15. H. Bouchriha, M. Schott, and J. L. Fave, *J. Physique*, **36**, 399 (1975).
16. P. Mark and W. Helfrich, *J. Appl. Phys.*, **33**, 205 (1962).
17. D. Blossey, *Phys. Rev.*, **B9**, 5183 (1974).
18. F. Willig, *Chem. Phys. Letters*, **40**, 331 (1976).
19. K. P. Charle and F. Willig, *Chem. Phys. Letters*, **57**, 253 (1978).
20. J. Kalinowski, J. Godlewski, and J. Gliniski, *J. Luminescence*, **17**, 467 (1978).
21. J. Gliniski, J. Godlewski, and J. Kalinowski, *Mol. Cryst. Liq. Cryst.*, **48**, 1 (1978).
22. C. F. Hackett, *J. Chem. Phys.*, **55**, 3178 (1971).
23. B. Sh. Barkhalov and Yu. A. Vidadi, *Thin Solid Films*, **40**, L5 (1977).
24. J. Singh and H. Baessler, *Phys. Stat. Solidi (b)*, **63**, 425 (1974).
25. J. Kalinowski, *Excitonic Interactions in Organic Molecular Crystals*, Zeszyt Naukowy Nr 266; Wydawnictwo Politechniki Gdańskiej, Gdańsk, Poland 1977 (in Polish).
26. E. Durand, *Electrostatique*, Ed. Masson et C<sup>ie</sup>, Paris, 1966.
27. J. Kalinowski and J. Godlewski, *Chemical Physics*, **32**, 201 (1978).
28. J. Godlewski, Thesis, Gdańsk 1976 (in Polish).

29. J. Kalinowski and J. Godlewski, *Phys. Stat. Solidi (b)*, **65**, 789 (1974).
30. J. Kalinowski and J. Godlewski, *Acta Physica Polonica*, **A46**, 523 (1974).
31. J. Godlewski and J. Kalinowski, *Phys. Stat. Solidi (a)*, **53**, 161 (1979).
32. J. Godlewski and J. Kalinowski, *Solid State Commun.*, **25**, 473 (1978).
33. Sh. D. Khan-Maghomatova, *Bull. Acad. Sci. U.S.S.R., Phys. Ser.*, **29**, 1326 (1966).
34. M. Pope and J. Burgos, *Mol. Cryst.*, **3**, 215 (1967).
35. J. O. Williams, *Sci. Prog., Oxf.*, **64**, 247 (1977).
36. J. Sworakowski, *Mol. Cryst. Liq. Cryst.*, **19**, 259 (1973).
37. K. Kojima, *Phys. Stat. Solidi (a)*, **51**, 71 (1979).
38. J. Godlewski, J. Gliński, and J. Kalinowski, Conference "Organische Festkörper," Poczdam, July 1979.
39. I. S. Grandshtain and I. M. Rizhik, Tables of Integrals, Sums, Series and Developments, *Gos. Izd. Fiz.-Mat. Lit.*, Moskva 1963.
40. M. E. Michel-Beyerle and R. Haberkorn, *Z. Naturf.*, **27a**, 1496 (1972).
41. H. P. Kallman and M. Pope, *J. Chem. Phys.*, **36**, 2482 (1962).
42. W. Mehl and J. M. Male, *Adv. Electrochemistry and Electrochemical Engng.*, **6**, 339 (1967).
43. R. Haberkorn and M. E. Michel-Beyerle, *Phys. Stat. Solidi (b)*, **67**, K 61 (1975).
44. R. M. Handy and L. C. Scala, *J. Electrochem. Soc.*, **113**, 109 (1966).
45. D. N. Jarrett and L. Ward, *J. Phys. D: Appl. Phys.*, **9**, 1515 (1976).

## Appendix A Calculation of the potential of linearly distributed charges

Calculation of the potential of linearly distributed point charges along the electrode at a distance  $D/2$  from electrode can be made on the basis of Eq. (5). For this case we have<sup>26</sup>

$$\varphi_i(x) = \frac{e}{4\pi\epsilon\epsilon_0} \left\{ \frac{1}{[y_i^2 + (x - D/2)^2]^{1/2}} - \frac{1}{[y_i^2 + (x + D/2)^2]^{1/2}} \right\} \quad (\text{A.1})$$

For  $x > D/2$  Eq. (A.1) can be approximated by

$$\varphi_i(x) \cong \frac{e}{4\pi\epsilon\epsilon_0} \frac{Dx}{(y_i^2 + x^2)^{3/2}}. \quad (\text{A.2})$$

In order to get the effective potential  $\varphi(x)$  at a distance  $x$  from the electrode, the sum

$$\varphi(x) = \sum_{i=1}^n \varphi_i(x) \quad (\text{A.3})$$

must be calculated. The sum of the series (A.3) cannot be presented as a simple mathematical formula. We have evaluated the sum (A.3) as a sum of

two components. The first one is calculated on the assumption  $y_i \ll x$ . Then (A.2) can be developed in a series†

$$\varphi_i(x) \cong \frac{e}{4\pi\epsilon\epsilon_0} \frac{D}{x^2} \left( 1 - \frac{3}{2} \frac{i^2 b^2}{x^2} \right) \quad (\text{A.4})$$

where  $y_i = ib_0$ , and  $i = 1, 2, \dots, y_0/b_0$ . The distance  $b_0$  is a mean distance between two charges (Figure 5). The second component of the sum is calculated for  $y_i > y_0$  in the approximation of a continuous charge distribution. It is only possible when

$$\frac{e}{4\pi\epsilon\epsilon_0} \frac{Dx}{(y_0^2 + x^2)^{3/2}} \cong \frac{\tau Dx}{4\pi\epsilon\epsilon_0} \int_{y_0}^{y_0 + b_0} \frac{dy}{(y^2 + x^2)^{3/2}}, \quad (\text{A.5})$$

where  $\tau = e/b_0$  = linear density of charge. Equation (A.5) is fulfilled when  $y \gg b_0$ . The evaluation of potential (A.3) will be done only for the case  $y_0 \gg b_0$  and  $y \ll x$ .‡ It results from the fact that in this case the potential of charge has a significant value compared to the image potential.

Finally, assuming that the number of charges tends to infinity, the potential can be represented by

$$\varphi(x) \cong 2 \frac{e}{4\pi\epsilon\epsilon_0} \sum_{i=1}^{y_0/b_0=N} \left[ \frac{D}{x^2} \left( 1 - \frac{3}{2} \frac{i^2 b^2}{x^2} \right) \right] + 2 \frac{\tau Dx}{4\pi\epsilon\epsilon_0} \int_{y_0}^{\infty} \frac{dy}{(y^2 + x^2)^{3/2}} \quad (\text{A.6})$$

The factor 2 originates from addition of two branches of linearly distributed charges. After a suitable mathematical treatment the expression (A.6) can be transformed into

$$\varphi(x) = \frac{\tau D}{2\pi\epsilon\epsilon_0 x} \left[ 1 - \frac{1}{4} \frac{b_0^3}{x^3} N(3N + 1) \right] \quad (\text{A.7})$$

For  $Nb_0 = y_0 \ll x$  Eq. (A.7) can be expressed by

$$\varphi(x) \cong \frac{\tau D}{2\pi\epsilon\epsilon_0 x} \quad (\text{A.8})$$

† Sums and integrals necessary for calculation presented in Appendixes are taken from.<sup>39</sup>

‡ For  $b_0 \gg x$  potential (A3) near the electrode is easily calculated applying Riemann's dzeta function. Namely:

$$\sigma(x) \cong 1,202, \dots, \frac{\tau D}{2\pi\epsilon\epsilon_0} \frac{x}{b_0^2}$$

In the approximation of a continuous charge distribution for all  $x$  the potential can be presented as:

$$\varphi_i(x) = \frac{\tau}{2\pi\epsilon\epsilon_0} \ln \left| \frac{(x + D/2)}{(x - D/2)} \right|. \quad (\text{A.9})$$

For  $x \gg D/2$  Eq. (A.9) merges with Eq. (A.8).

## Appendix B Calculation of the potential of a planar distribution of charges

Let us assume, that the charge is planarly distributed near the electrode at a distance  $D/2$  from it and the surface density of charge is equal  $\sigma = e/c_0^2$ , where  $c_0$  is a mean distance between the nearest neighbour charges (Figure 6). The distance between the  $i$ -th charge and the escaping charge is

$$y_i = (n^2 c_0^2 + k^2 c_0^2)^{1/2} = y_{n,k}. \quad (\text{A.10})$$

Applying a similar procedure to that of Appendix A, the total potential can be written as

$$\begin{aligned} \varphi(x) = & \sum_{i=1}^{(\pi y_0^2/c_0^2 - 1)} \frac{e}{4\pi\epsilon\epsilon_0} \frac{D}{x^2} - 4 \cdot \frac{3}{8} \frac{e}{\pi\epsilon\epsilon_0} \left[ \sum_{n=1}^{y_0/c_0=N} \frac{Dc_0^2}{x^4} n^2 + \sum_{k=1}^{y_0/c_0=N} \frac{Dc_0^2}{x^4} k^2 \right] \\ & + \frac{\sigma Dx}{4\pi\epsilon\epsilon_0} \int_{y_0}^{\infty} \frac{2\pi y dy}{(y^2 + x^2)^{3/2}}. \end{aligned}$$

The approximation of a continuous charge distribution for the last component of sum (A.11) can be applied when

$$\frac{e}{4\pi\epsilon\epsilon_0} \frac{Dx}{(y_0^2 + x^2)^{3/2}} \cong \frac{\sigma Dx}{4\pi\epsilon\epsilon_0} \int_{y_0}^{y_0+d_0} \frac{2\pi y dy}{(y^2 + x^2)^{3/2}}. \quad (\text{A.12})$$

Here  $2\pi\sigma y_0 d_0 = e$  and  $2\pi y_0 d_0$  is the surface containing one charge. The Eq. (A.12) is fulfilled for  $y_0 \gg d_0$ . It means, that there are at least a dozen or so charges at a distance  $y_0$  from the escaping charge. For this case the Eq. (A.11) can be presented in approximate form

$$\varphi(x) \cong \frac{\sigma D}{2\epsilon\epsilon_0} \left( 1 - \frac{c_0^2}{2x^2} - \frac{c_0^2}{\pi x^2} N(N+1)(2N+1) + \frac{3}{8} \frac{N^4 c_0^2}{x^4} \right). \quad (\text{A.13})$$

In order to obtain the potential in this approximation it should not depend on  $N$

$$\frac{d\varphi(x)}{dN} = 0 \quad (\text{A.14})$$



Then, from (A.13) and (A.14) we can get an approximate expression for the potential

$$\varphi(x) \cong \frac{\sigma D}{2\epsilon\epsilon_0} \left[ 1 - \frac{c_0^2}{2x^2} - 3.55 \frac{c_0^2}{x^4} \right] \quad (\text{A.15})$$

For large  $x$  Eq. (A.15) can be transformed into

$$\varphi = \frac{\sigma D}{2\epsilon\epsilon_0} \quad (\text{A.16})$$

This is in accordance with the potential of continuous charge distribution.